J Appl Electrochem (2007) 37:1447–1454
DOI 10.1007/s10800-007-9352-y

ORIGINAL PAPER

Realising a reference electrode in a polymer electrolyte fuel cell by laser ablation

Dietmar Gerteisen

Received: 13 November 2006 / Revised: 18 June 2007 / Accepted: 18 June 2007 / Published online: 3 July 2007

Abstract This work presents a new concept for realising a reference electrode configuration in a PEM fuel cell by means of laser ablation. The laser beam is used to evaporate a small part of the electrode of a catalyst-coated membrane (CCM) to isolate the reference electrode from the active catalyst layer. This method enables the simultaneous ablation of the electrodes on both sides of the CCM because the membrane is transparent for the laser beam. Therefore, a smooth electrode edge without electrode misalignment can be realised. A test fuel cell was constructed which together with the ablated CCM enables the separation of the total cell losses during operation into the cathode, anode and membrane overpotentials in PEFC as well as in DMFC mode. The methanol tolerance of a selenium-modified ruthenium-based catalyst ($RuSe_x$) was investigated under real fuel cell conditions by measuring polarisation curves, electrochemical impedance spectroscopy (EIS) and current interrupt measurements (CI).

Keywords PEMFC · DMFC · Methanol-tolerant catalyst · Reference electrode · Current interrupt measurements · Electrochemical impedance spectroscopy

1 Introduction

The high-energy content of liquid methanol, a simple storage and simple refilling make direct methanol fuel cells (DMFC) a promising candidate for portable power applications. However, there are several serious technical problems to overcome for such cells to be competitive in the market. The thermodynamic reversible cell potential for the overall cell reaction of a DMFC is 1.21 V at 298 K [1]. However, the open circuit voltage (OCV) is typically only in the range 600–750 mV [2–5]. This large overpotential is caused by methanol crossover from the anode to the cathode side, where methanol is oxidising on the platinum catalyst and consequently causing a mixed potential [2, 5–9]. To avoid the oxidation of methanol on the cathode several methods have been explored. Possibilities are the development of a novel membrane that prevents the permeation of methanol through the membrane [10, 11] or the use of methanol vapour instead of a liquid methanol solution to reduce the amount of dissolved methanol in water at the electrode/membrane interface [12] and therefore the diffusive flux of methanol to the cathode. Another approach to overcome the decrease in cathode performance by methanol crossover is to use a methanol tolerant oxygen reduction electrocatalyst, i.e., an oxygen reduction reaction (ORR) selective catalyst [7, 9, 13–15]. High methanol tolerance is reported in the literature for non-noble metal catalysts based on chalcogenides and macrocycles of transition metals or platinum-based binary alloyed catalysts [14]. Investigations of the electrocatalytic activity of such catalysts using rotating disc electrode (RDE) measurements in acidic media show cathode potentials up to 1 V [14, 15]. Nevertheless, the OCV of technical electrodes with methanol tolerant cathode catalysts in DMFCs do not show such high values. Thus, either the anode potential of the methanol oxidation reaction (MOR) is far above the theoretical value of approx. 20 mV [1] or a so far not completely understood coupling between the cathode and anode causes this low OCV despite of a methanol tolerant catalyst.

D. Gerteisen (✉)
Fraunhofer Institute for Solar Energy Systems, Heidenhofstr. 2, 79110 Freiburg, Germany
e-mail: dietmar.gerteisen@ise.fraunhofer.de

Under real fuel cell conditions it is difficult to investigate the influence of methanol on the cathode performance and the coupling of the electrodes, respectively, without having a reference electrode (RE) configuration in the cell. Recently, several papers have been published about reference electrodes in a fuel cell. Some of these publications focus on modelling the influence of the position of the reference electrode [16–18]. It was found that a misalignment of the working and counter electrodes in the range of a few microns (depending on the membrane thickness) results in a highly asymmetric potential distribution near the electrode edges in the membrane, causing an unknown potential shift of the reference electrode towards the overhanging electrode. Additionally, this shift depends on the current applied to the cell, which leads to significant errors in electrochemical impedance spectroscopy (EIS) measurements. An exact alignment is necessary for the reference electrode to contact a current independent potential in the centre of the membrane. This makes the preparation of a catalyst-coated membrane (CCM) including a reference electrode very difficult and hardly feasible. Thus, few publications can be found presenting a reference electrode configuration in a fuel cell [16, 19, 20] to determine polarisation data of the cathode and anode. Due to the higher requirements on the reference electrodes for EIS measurements only one paper presents impedance spectra [21].

This work demonstrates a completely new concept for a state-of-the-art prepared CCM (even a commercially available CCM is possible) that will be treated by laser ablation to produce a reference electrode on the same membrane. This technique allows partial electrical insulation of the electrodes by evaporation of a small isolation gap with a laser beam. The segmented part can be used as a reference electrode. By means of this reference electrode configuration in a test cell the performance of a methanol tolerant ruthenium-based catalyst modified with selenium ($RuSe_x$) was investigated using polarisation curves, EIS measurements and current interrupt measurements (CI).

2 Experimental

2.1 Preparation of reference electrodes

The preparation of the CCMs generally follows a standard procedure. For the anode side a PtRu/XC72 catalyst from Johnson Matthey (HiSpec10000) was used. For the cathode side 40w%$RuSe_x$ on 60w%XC72 was used. The catalyst ink was pasted on a decal foil and then hot pressed on a Nafion 117. The catalyst loadings for the investigated CCMs can be found in Table 1. A carbon cloth from E-Tek (thickness 350 μm) with a micro porous layer (40%PTFE/60%VulcanXC72, thickness 80 μm) was used as gas diffusion layer for all experiments. Starting from the prepared CCM the catalyst layer is removed at the boundary of the working (WE) and counter electrode (CE), respectively, and the reference electrodes (RE) by laser ablation. Thus, a CCM with electrically isolated catalyst layer regions is obtained (Fig. 1).

Table 1 Catalyst loadings of the investigated CCMs

No.	Cathode		Anode	
	Catalyst	Loading (mg cm^{-2})	Catalyst	Loading (mg cm^{-2})
CCM #1	$RuSe_x$	0.9	Pt/Ru	2.0
CCM #2	$RuSe_x$	0.6	Pt/Ru	0.5
CCM #3	$RuSe_x$	1.26	Pt/Ru	1.9
CCM #4	Pt	1	Pt/Ru	3.0

The CCM laser ablation was carried out with a Nd:YAG-LASER ('Rofin Sinar Laser GmbH') operating at a wavelength in the near infrared of 1,049 nm. Due to the high adsorption values of the carbon supported catalyst and the fact that the membrane is transparent to the laser beam, the catalyst layers are very effectively removed on both sides simultaneously without damaging the membrane. The laser beam burns a gap of about 30 μm in the catalyst layers. To ensure sufficient isolation between WE/CE and RE and to avoid edge effects of the potential distribution in the membrane to the reference potential the laser ablation was repeated 10 times with a small offset of 10 μm. An isolation gap of 300 μm was reached (Fig. 1a). By means of this technique sharp electrode edges with an exact alignment of the cathode and anode catalyst layers (Fig. 1b) can be realised which would not be possible with conventional electrode preparation methods. A detailed discussion of MEA laser ablation can be found in [22].

2.2 Test cell and bench

The CCM treated by laser ablation was sandwiched between two gas diffusion layers with micro porous layers. The current collectors were made of titanium. Figure 2 shows the single channel flow field milled in the current collector with a geometric area of 1 cm^2. The cell temperature was controlled by water channels inside the titanium block connected to a cryostat (Fisherbrand FBC 720). The cell temperature was measured by a thermocouple 1 mm above the flow channel in the titanium plate on the cathode side. The contacts to the laser ablated reference electrodes were realised by a gold wire positioned on the gas/fuel outlet of the cell, approximately 2 mm from the working/counter electrodes. The gold wire was wound like a spring to achieve a good and stable contact to the electrodes even when the membrane was swelling or shrinking. Note that the reference electrode on the anode side and

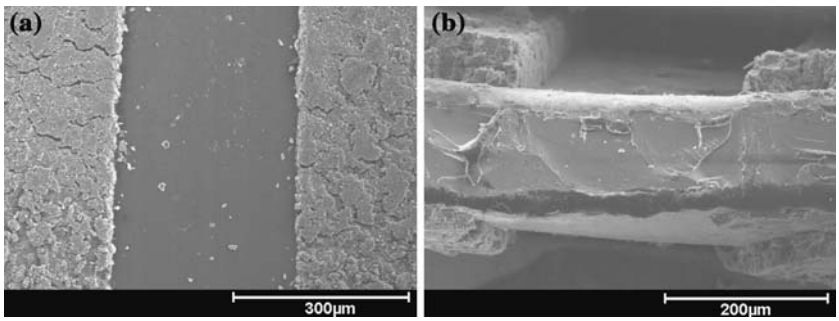

Fig. 1 (**a**) Top view of the ablated CCM: an isolation gap of about 300 µm with sharp electrode edges is reached. Only a few particles are left on the membrane. (**b**) Profile view: the electrode edges are exactly on top of each other

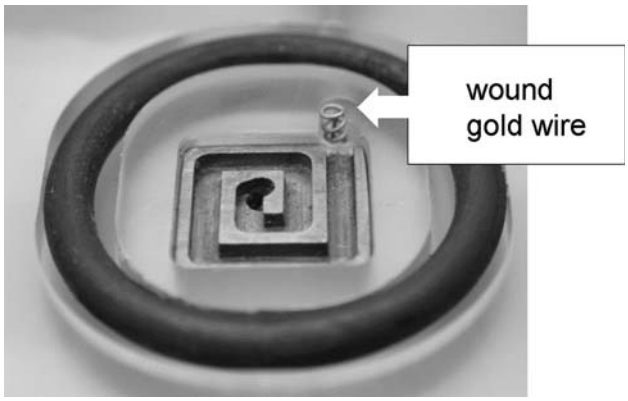

Fig. 2 The contact to the reference electrode is realised by a wound gold wire at the gas/fuel outlet of the cell

cathode side is in the same reactant compartment as the WE and CE, respectively. Therefore, the potential of the reference electrode on the cathode side is not that of a normal hydrogen electrode (NHE) but the equilibrium potential of the ORR and the potential of the reference electrode on the anode side is the equilibrium potential of the MOR. The advantage of this configuration is that the reference electrodes are located as close as possible to the WE/CE because no sealing is necessary to separate different reactant compartments. Disadvantageous is the fact that the absolute values of the potentials (referred to the NHE) cannot be measured and therefore poisoning of the reference electrodes can impact the potential measurements. This problem is discussed in the next section. Figure 3 schematically shows an ablated CCM. The five measurable voltages (V1–V5) and impedances (Z1–Z5) are illustrated. The equipotential lines of an ideal symmetric electrode alignment and homogeneous conductivity of the membrane are pictured. The electrical potentials of the REs (Φ^e_{ra}, Φ^e_{rc}) are connected via the phase boundary to the protonic potential level in the middle of the membrane.

A SOLARTRON 1286 in combination with a SOLARTRON 1250 frequency response analyser (FRA) was used for electrochemical measurements. The current and cell potential were recorded by the load itself. The cathode overpotential ($\eta_c = \Phi^e_c - \Phi^e_{rc}$,) the anode overpotential ($\eta_a = \Phi^e_a - \Phi^e_{ra}$) and the voltage difference of the REs ($U_{OC,R} = \Phi^e_{rc} - \Phi^e_{ra}$) were measured with a Datalogger (HP 34970A). The electrochemical impedance spectra were recorded in the frequency range 100 mHz to 10 kHz. The current interrupt measurements were carried out using a KEPCO load (BOP 20-5M), whereas the potential

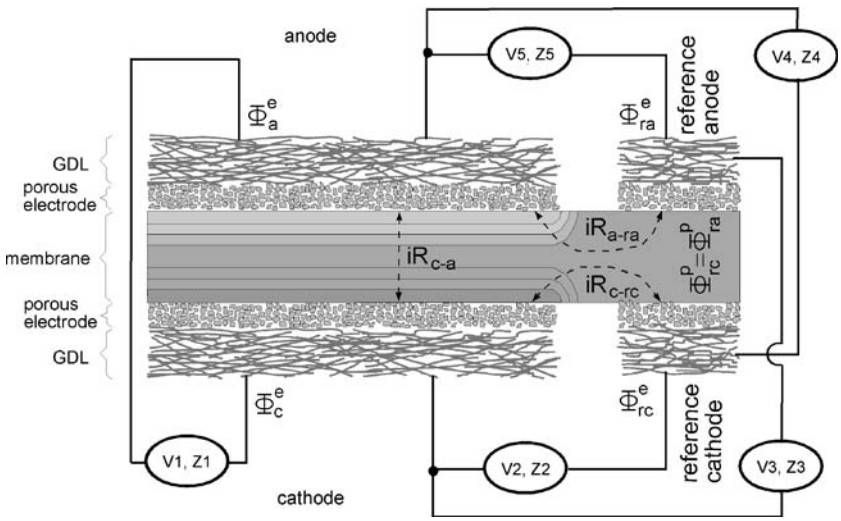

Fig. 3 Schematic diagram of an ablated CCM. Five different voltages and impedances are measurable

relaxations were recorded on a digital oscilloscope (TEKTRONIX TDS3014B). The abrupt current interruption was realised by releasing a fast protect switch. The gas flow was regulated with gas flow controllers (Bronkhost) and was humidified by passing each gas stream through an external tempered humidifier. Temperatures of gas lines between humidifier and cell were maintained 5 °C above the humidifier temperature to avoid condensation. A pump (HPLH20/200-PF, Ingenieurbüro CAT) was employed to supply aqueous methanol solution from a reservoir.

3 Results and discussion

First, a proof of concept of the laser ablation for isolating reference electrodes from a CCM is given. Figure 4a shows a polarisation curve of the DMFC (CCM #1) together with the cathode and anode overpotentials. Additionally, the voltage difference between both reference electrodes ($U_{OC,R} = \Phi^e_{rc} - \Phi^e_{ra}$) is pictured, which shows a stable potential under load of about 610 mV. The cathode overvoltage is corrected by the *iR*-drop whereas the resistance is taken by the high frequency resistance (HFR: 10 kHz) measured from the cathode (CE) to the cathode reference electrode (see Fig. 2). The anode overvoltage is also corrected by the *iR*-drop measured from the anode (WE) to the anode reference electrode. For this operating condition the activation overpotential of the ORR is about twice as large as the overpotential of the MOR. The open circuit voltage is about 605 mV (close to $U_{OC,R}$). Polarisation curves of CCM #2 fed with hydrogen as fuel are depicted in Fig. 4b. The measurements show a higher OCV (875 mV) and a higher limiting current density. The reference potentials are also stable but $U_{OC,R}$ only reaches a value of about 820 mV. An explanation for this could be that the reference electrodes have never been under load and therefore the catalyst is not completely activated or is in oxidized state which would cause a lower $U_{OC,R}$. The activation overpotential of the hydrogen oxidation reaction (HOR) is negligible compared to the ORR. The results of the steady state measurements show that oxygen, as well as methanol, generates a stable reference potential. An isolation gap of 300 μm in case of a Nafion 117 is large enough for the REs not to be influenced by edge effects from the WE/CE.

Figure 5a shows impedance spectra of CCM #1 at a cell potential of 50 mV (T_{cell} = 51 °C) using an aqueous methanol solution (1 M) as fuel. Both small impedance loops are anode spectra: Z4 is measured versus the cathode reference electrode and Z5 is measured versus the anode reference electrode (see Fig. 2). The diameter of the loops are equal, indicating that both reference electrodes are stable for EIS measurements. Z2 and Z3 are the cathode impedance spectra referring to the two different reference electrodes. Their diameters are also the same. The addition of the measured anode and cathode impedance spectra (Z3 + Z5) results in the measured total cell impedance. This result is a good proof for time stability of the REs (measuring all five spectra one after another needs about 10 min).

Figure 5b shows impedance spectra of CCM #2 at a cell potential of 600 mV (T_{cell} = 41 °C) with hydrogen as fuel. As opposed to the DMFC the anode impedance of a PEFC is small compared to the cathode impedance. The anode impedance shows an inductive behaviour in the low frequency range. Explanations for this fact could be the ad-/desorption process of hydrogen molecules on the active sites or the water dependence of the electrode performance [23, 24].

Despite nearly perfect electrode alignment the high frequency resistances (HFR) of the anode and cathode spectra differ both in DMFC and in PEFC measurements. This means that the reference electrodes do not contact the electrolyte potential in the middle of the membrane with a symmetrical potential distribution such as depicted in Fig. 6a. The simulation shows that a non-homogeneous membrane conductivity (δ) due to a gradient in the

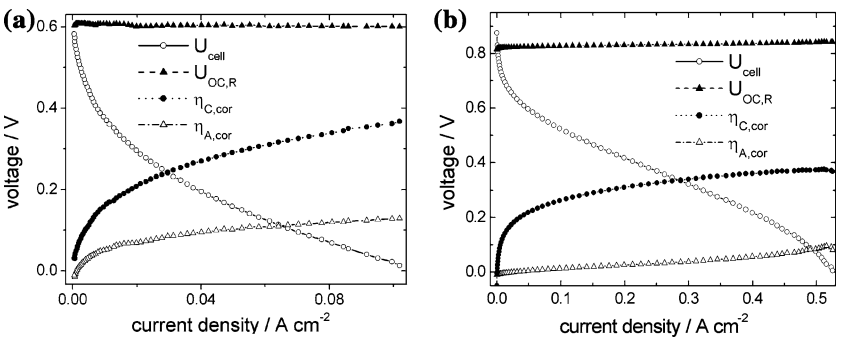

Fig. 4 Measured polarisation curves of the cell (Ucell), the OCV between the two reference electrodes ($U_{OC,R}$), absolute value of cathode and the anode overpotential during a sweep measurement: (**a**) methanol is used as fuel, $\dot{V}_{MeOH} = 2\,\text{ml min}^{-1}$, $\dot{V}_{O_2} = 12\,\text{ml min}^{-1}$, T_{cell} = 71 °C; (**b**) hydrogen is used as fuel, $\dot{V}_{H_2} = 8\,\text{ml min}^{-1}$, $\dot{V}_{O_2} = 12\,\text{ml min}^{-1}$, T_{cell} = 41 °C

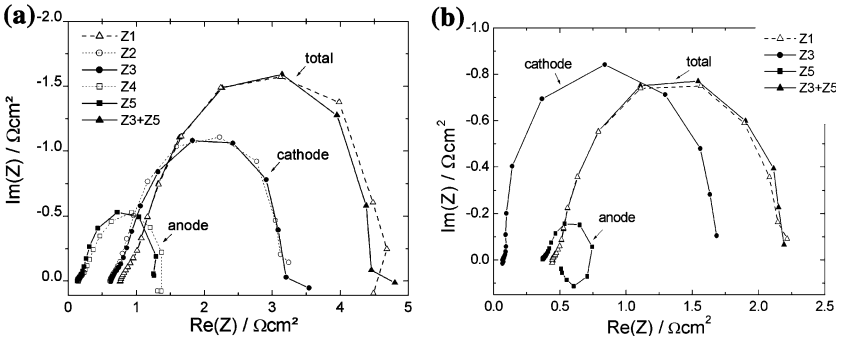

Fig. 5 (**a**) Impedance spectra at a cell voltage of 50 mV of the total cell (Z1), the cathode (Z2, Z3) and the anode (Z4, Z5) with methanol as fuel. (**b**) Impedance spectra at a cell voltage of 600 mV of the total cell (Z1), the cathode (Z3) and the anode (Z5) with hydrogen as fuel. The summation of the cathode and anode impedance (Z3 + Z5) results in the total cell impedance (Z1) in both cases

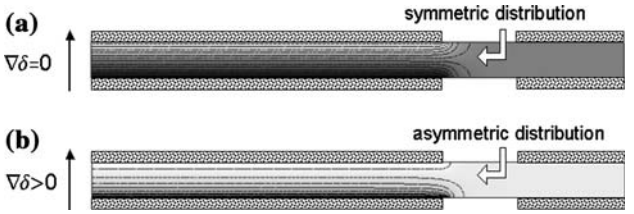

Fig. 6 Simulated potential distribution in a membrane with (**a**) homogeneous conductivity, (**b**) a linear increasing conductivity from bottom to top

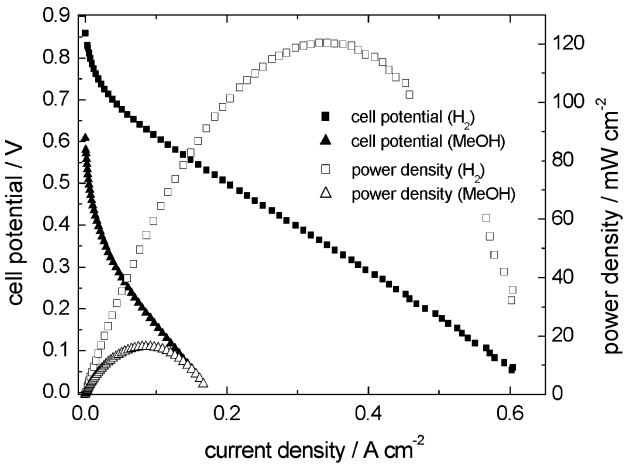

Fig. 7 Comparison of the performance of the $RuSe_x$-cathode catalyst (CCM #3) between hydrogen ($\dot{V}_{H_2} = 8\,\text{ml min}^{-1}$, $T_{cell} = 64\,°C$) and methanol ($\dot{V}_{MeOH} = 2\,\text{ml min}^{-1}$, $T_{cell} = 83\,°C$) as fuel. In both cases the oxygen flow rate was $\dot{V}_{O_2} = 12\,\text{ml min}^{-1}$. Changing from hydrogen to methanol shows a drastic decrease of the performance

membrane water content results in an asymmetrical potential distribution even with a perfect electrode alignment (Fig. 6b). Therefore, HFR_{anode} is smaller than HFR_{cath} in DMFC measurements due to the aqueous methanol solution humidifying the anode side very well. In PEFC measurements it is vice versa due to the higher water content on the cathode side from the product water of the ORR and the electroosmotic drag.

Impedance spectra at different cell potentials indicate a constant ratio of the HFR_{anode} to $HFR_{cathode}$. This means that the asymmetrical potential distribution is not affected by the applied current and therefore does not disturb the EIS measurements.

Figure 7 shows two polarisation curves of the CCM #3. First the cell was operated with methanol (1 M) as fuel before switching to hydrogen as fuel. It is obvious that the PEFC shows much better performance. An increase of the OCV from 610 mV to 860 mV is observed, which leads to an increase of the peak power density from 16.4 mW cm^{-2} to 120 mW cm^{-2}. The huge difference in OCV remains unexplained because the methanol tolerant $RuSe_x$-catalyst should not be sensitive towards methanol permeation. A closer look at the polarisation curve of the cathode potential for both measurements (Fig. 8) shows that the activation overpotentials differ slightly. The cathode overpotential of the methanol-driven cell is slightly higher than that of the PEFC. It is assumed that an additional mass transport limitation in the porous gas diffusion electrode due to the presence of permeated liquid methanol/water solution could cause this difference.

In Fig. 9 the cell impedance spectra of CCM #3 at a current density of 0.033 A cm^{-2} in DMFC and PEFC mode is shown. Due to better membrane humidification the high frequency resistance of the DMFC is lower than that of the PEFC, but shows a significantly larger impedance loop. The measured cathode impedance of the DMFC (Fig. 10a) differs moderately from that of the PEFC. The loop is slightly enlarged which can be explained by the same effect as discussed for the overpotential curve above: the aqueous methanol solution blocks the active sites and finally leads to additional mass transport limitations. A parasitic MOR on the cathode can be excluded. A large difference is measured in the anode impedance (Fig. 10b). In contrast the impedance of the hydrogen-driven anode is negligible compared to the methanol-driven anode.

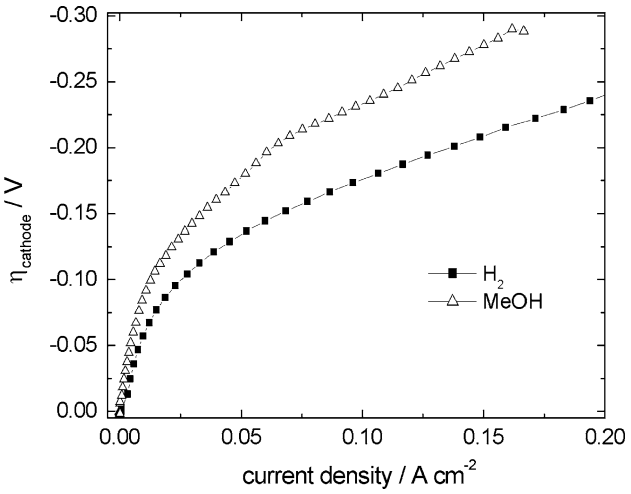

Fig. 8 The steeper increase of the cathode overpotential if methanol is used as fuel could be explained by flooding due to permeated aqueous methanol solution causing a limitation for the oxygen diffusion to the active sides

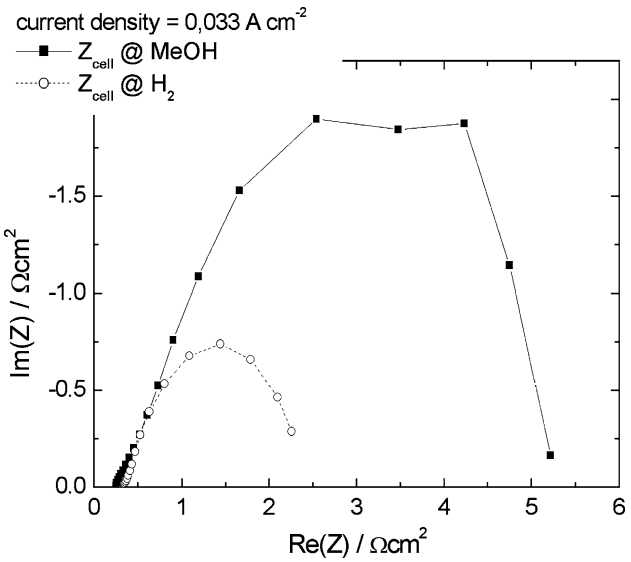

Fig. 9 Measured cell impedance spectra in PEFC ($\dot{V}_{H_2}$ = 8 ml min^{-1}, T_{cell} = 65 °C) and DMFC ($\dot{V}_{MeOH}$ = 2 ml min^{-1}, T_{cell} = 81 °C) mode. In both cases the oxygen flow rate was $\dot{V}_{O_2}$ = 12 ml min^{-1}

3.1 Methanol tolerance of $RuSe_x$

The investigation of methanol tolerance of a catalyst is easy to carry out in half cell measurements in liquid electrolyte because the potential of the working electrode is measurable versus a reference electrode and the potential of the investigated electrode is not affected by the counter electrode. Under real fuel cell conditions the measurable cell voltage depends on both electrode potentials (WE/CE) influencing each other (e.g., methanol crossover), therefore the potential difference between the cathode and the anode at open circuit is not a good measure for the methanol tolerance of a catalyst.

One possibility to investigate the methanol tolerance of the cathode catalyst is to measure the cathode exhaust. If there is a large amount of carbon dioxide (CO_2) in the exhaust gas, a high methanol oxidation reaction rate on the cathode can be concluded, since CO_2 is the product of the MOR. A problem of this measurement technique is diffusion of CO_2 from the anode side through the membrane. Therefore, CO_2 is always present in the cathode gas compartment, which has to be considered. In several publications an overshoot of the cell voltage is measured if there is a sudden load step from a high current to a low current. In most cases the phenomenon is discussed as an interaction between the relaxation of the ORR potential and the methanol crossover building a mixed potential on the cathode side [8, 25, 26]. Thus, we used the current interrupt technique to prove the methanol tolerance of the $RuSe_x$-catalyst with the reference electrode configuration. Figure 11 shows the cathode potential relaxation of two different CCMs. A current density of 100 mA cm^{-2} was applied before the load suddenly switched off. One CCM is prepared with Pt/C (CCM #4) as cathode catalyst while the other CCM is prepared with $RuSe_x$/C (CCM #3). Pt/Ru is used as anode catalyst for both CCMs. The curve with the Pt-catalyst shows an overshoot behaviour of the cathode potential (grey line), while the $RuSe_x$-based CCM does not show such a behaviour (black line). This is good evidence for the methanol tolerance of the $RuSe_x$-catalyst.

However, the measured cell voltage of the $RuSe_x$-based CCM also shows an overshoot behaviour (Fig. 12). By means of the reference electrode configuration this overshoot of the cell potential can be clearly attributed to an undershoot of the anode potential. This means that on the anode side there are at least two processes with two different time constants competing with one another. The faster process is responsible for the anode potential decrease to a low potential (favourable for fuel cell application), the second process after some seconds (approx. 6 s) forces the anode potential to an adverse high potential. The undershoot behaviour of the anode relaxation curve leads to the conclusion that the anode potential at steady state is at least 100 mV higher as expected from the theory. This assumption cannot be proven with the used reference electrode configuration because the absolute value of the REs are unknown. Here, a hydrogen reference electrode is essential. The increased anode potential consequently results in a low cell voltage even if a methanol tolerant catalyst is used. Figure 13 shows the dependence of the anode potential relaxation on the load current and methanol concentration. Starting from a load current of 0.01 and 0.04 A, respectively, the anode potential relaxation was

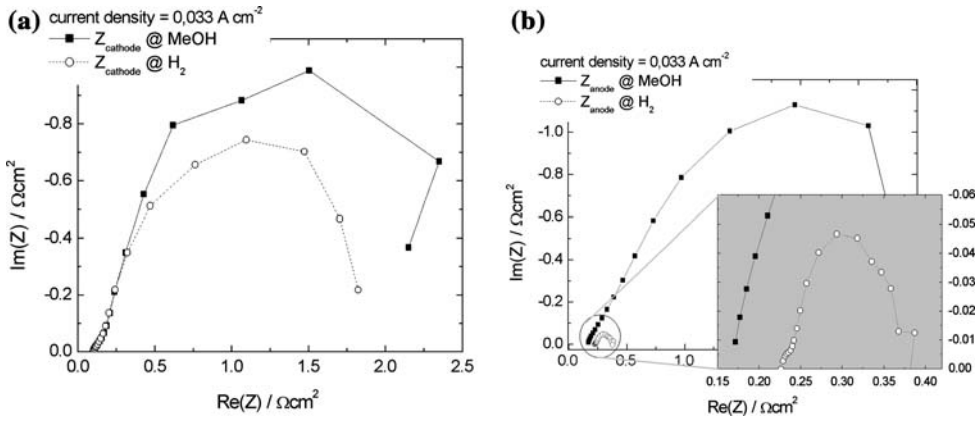

Fig. 10 (**a**) Cathode impedance spectra in PEFC and DMFC mode. With methanol as fuel the loop of the impedance spectrum is a little bit larger than with hydrogen as fuel. (**b**) The loops of anode impedance spectra are completely different in their size

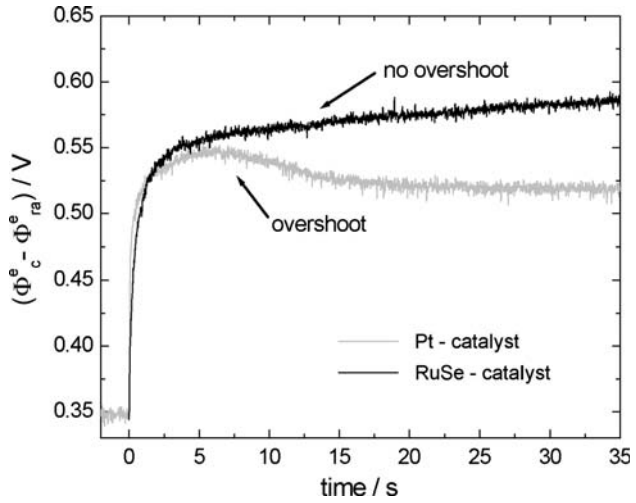

Fig. 11 The cathode polarisation relaxation curve after current interruption of a Pt-based electrode shows an overshoot behaviour due to methanol crossover and the consequential mix potential. The $RuSe_x$-based electrode do not show such overshoot behaviour, which can be interpreted as a positive proof of the methanol tolerance of this catalyst. ($\dot{V}_{MeOH,1\,M} = 2\,ml\ min^{-1}$, $\dot{V}_{O_2} = 12\,ml\ min^{-1}$, $T_{cell} = 81\ °C$)

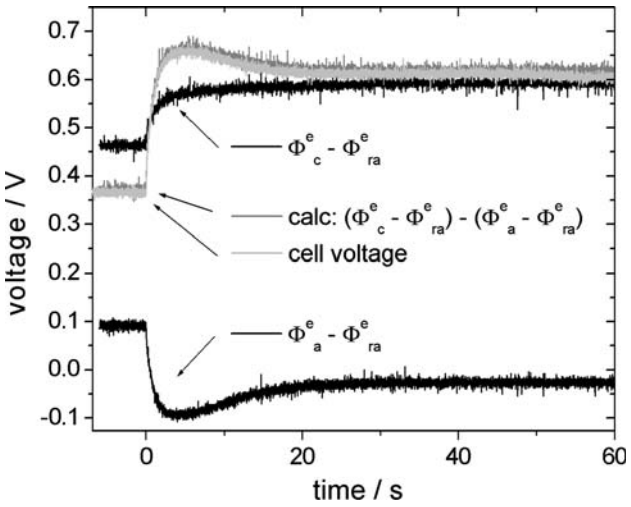

Fig. 12 A large undershoot behaviour can be measured of the anode potential after current interruption resulting in a overshoot behaviour of the cell voltage. ($RuSe_x$-catalyst, $\dot{V}_{MeOH,1\,M} = 2\,ml\ min^{-1}$, $\dot{V}_{O_2} = 12\,ml\ min^{-1}$, $T_{cell} = 81\ °C$)

measured with two different methanol concentrations (0.5 and 3 M). The curves show clearly that a higher load current results in larger undershoot. The relaxation curves with 0.5 M methanol solution reach steady state after approximately 14 s, while the relaxation curves with 3 M methanol solution do not reach steady state within 30 s. The origin of the undershoot can be poisoning effects of the anode by intermediates such as CH_2OH, CHOH, CHO or CO described in [8, 12]. For a qualitative conclusion concerning the behaviour of the anode further experimental investigations have to be conducted.

4 Conclusion

A new concept for realising a reference electrode configuration in a polymer electrolyte fuel cell is presented. By means of a laser ablation technique a selected part of the electrodes (cathode/anode) of a state-of-the-art CCM was electrically isolated and used as a reference electrode. It was shown that oxygen, as well as methanol, generates a stable reference potential for steady-state measurements and dynamic measurements such as electrochemical impedance spectroscopy and current interrupt measurements. The separation of the cathode and anode losses for a PEFC, as well as a DMFC, is practicable. The performance of a selenium-modified ruthenium-based ($RuSe_x$) cathode catalyst was investigated under real fuel cell conditions. Polarisation curves and impedance spectra of the $RuSe_x$-catalyst based electrode show the same cathode performance for both hydrogen and methanol as fuel. In DMFC mode, the missing overshoot behaviour of the cathode potential after current interruption indicates the methanol tolerance of the $RuSe_x$-catalyst. Nevertheless, it was found that despite the methanol tolerance of the cathode catalyst there is a large difference in the OCV depending on

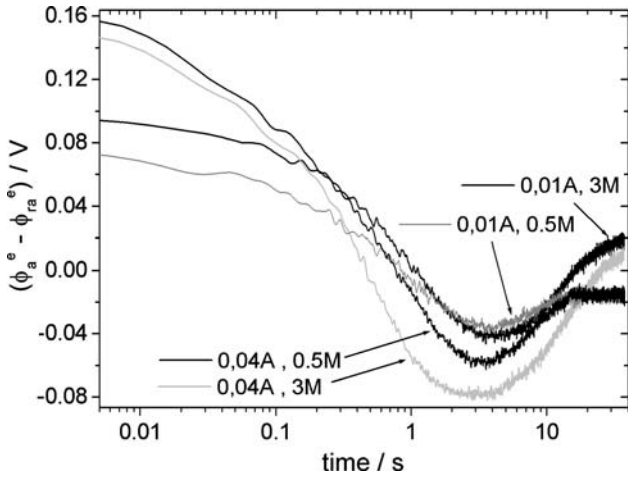

Fig. 13 The amplitude and the relaxation time of the undershoot of the anode potential depends on the load current as well as on the methanol concentration. ($RuSe_x$-catalyst, $\dot{V}_{MeOH,1\,M} = 2\,ml\ min^{-1}$, $\dot{V}_{O_2} = 12\,ml\ min^{-1}$, T_{cell} = 81 °C)

whether methanol or hydrogen is used as fuel. The relaxation curve of the anode potential shows a strong undershoot behaviour (up to 100 mV), which cannot be fully explained. It is assumed that there is a strong influence of CO poisoning (or other intermediates) on the anode potential that also causes the lower OCV. Due to the lack of reference electrodes in fuel cells many researchers publishing dynamic DMFC measurements overestimate the influence of methanol crossover building a mixed potential on the cathode (responsible for the low OCV). The explanation for the overshoot behaviour of the cell voltage after load change is, in most cases, completely explained by the methanol crossover which can be excluded by our measurements. The anode potential clearly shows an undershoot behaviour. By means of the reference electrode configuration it can be shown that the high anode potential (poisoning effect) at steady state has a strong impact on the low cell voltage of a DMFC. Finally, it can be concluded that a reference electrode configuration is necessary in order to distinguish losses of the anode and cathode for examining coupled phenomena, which is not possible in half cell measurements often carried out for DMFC.

Acknowledgements This work was financially supported by the Bundesministerium für Bildung und Forschung (BMBF) under contract No. 03SF0302. Special thanks goes to Dr. S. Fiechter from HMI Berlin for the supply of $RuSe_x$-catalyst and Dr. K. Wippermann from RC Juelich for preparing the CCM samples.

References

1. Iwasita T (2003) In: Vielstich W, Gaststeiger H, Lamm A (eds) Handbook of fuel cells, vol 2. Wiley, Chichester, pp 603–624
2. Paganin VA, Sitta E, Iwasita T, Vielstich W (2005) J Appl Electrochem 35:1239
3. Dohle H, Jung R, Kimiaie N, Mergel J, Müller M (2003) J Power Sources 124:371
4. Zhao X, Fan X, Wang S, Yang S, Yi B, Xin Q, Sun G (2005) Int J Hydrogen Energy 30:1003
5. Silva V, Schirmer J, Reissner R, Ruffmann B, Silva H, Mendes A, Madeira L, Nunes S (2005) J Power Sources 140:41
6. Eickes C, Piela P, Davey J, Zelenay P (2006) J Electrochem Soc 153(1):A171
7. Lee K, Savadogo O, Ishihara A, Mitsushima S, Kamiya N, Ota K (2006) J Electrochem Soc 153(1):A20
8. Krewer U, Sundmacher K (2005) J Power Sources 154:153
9. Scott K, Shukla A, Jackson C, Meuleman W (2004) J Power Sources 126:67
10. Jörisson L, Gogel V, Kerres J, Garche J (2002) J Power Sources 105:267
11. Jiang R (2006) J Electrochem Soc 153(8):A1554
12. Kallo J, Kamara J, Lehnert W, von Helmolt R (2004) J Power Sources 127:181
13. Tributsch H, Bron M, Hilgendorff M, Schulenburg H, Dorbandt I, Eyert V, Bogdanoff P, Fiechter S (2001) J Appl Electrochem 31:739
14. Koffi R, Coutanceau C, Garnier E, Léger JM, Lamy C (2005) Electrochim Acta 50:4117
15. Yang H, Coutanceau C, Léger JM, Alonso-Vante N, Lamy C (2005) J Appl Electrochem 576:305
16. Adler S, Henderson B, Wilson M, Taylor D, Richards R (2000) Solid State Ionics 134:35
17. Liu Z, Wainright JS, Huang W, Savinell RF (2004) Electrochim Acta 49:923
18. Nagata M, Itoh Y, Iwahara H (1994) Solid State Ionics 67:215
19. He W, Van Nguyen T (2004) J Electrochem Soc 151(2):A185
20. Siroma Z, Kakitsubo R, Fujiwara N, Ioroi T, Yamazaki SI, Yasuda K (2006) J Power Sources 156:284
21. Li G, Pickup P (2004) Electrochim Acta 49:4119
22. Schmitz A, Wagner S, Hahn R, Weil A, Schneiderlöcher E, Tranitz M, Hebling C (2004) Fuel Cells 4(3):1
23. Wiezell K, Gode P, Lindbergh G (2006) J Electrochem Soc 153(4):A749
24. Wiezell K, Gode P, Lindbergh G (2006) J Electrochem Soc 153(4):A759
25. Argyropoulos P, Scott K, Taama W (2000) J Power Sources 87:153
26. Argyropoulos P, Scott K, Taama W (2000) Electrochim Acta 45:1983